APPLICATION OF STRONG FLUCTUATION THEORY TO MICROWAVE EMISSION FROM DRY SNOW

H. Wang, J. Pulliainen, and M. Hallikainen

Laboratory of Space Technology
Helsinki University of Technology
P. O. Box 3000, 02015, HUT, Finland

Abstract–This study is concerned with the development of a model to describe microwave emission from dry snow cover. The model is based on the radiative transfer and the strong fluctuation theory. In the model, a spherical symmetric correlation function with an exponential form is used to describe the random permittivity fluctuations. The phase matrix and extinction coefficient of snowpack for a spherical symmetric correlation function are obtained by employing the strong fluctuation theory. The vector radiative transfer equation for a layer of a random medium is solved by using Gaussian quadrature and eigen analysis. Comparisons with brightness temperature data at 5, 10.7, 18, 37 GHz are made. It is shown that the model fits the experimental data by using physical parameters of the dry snow as obtained from ground truth measurements.

1. Introduction
2. Formulation
3. Comparison with Other Modelling Approaches and Experimental Data
4. Conclusions
Appendix. The Derivation of Parameter $W_{\alpha,\beta}$
References

1. INTRODUCTION

Theoretical modelling in passive remote sensing deals with the brightness temperature or emissivity of a target. A number of emission

models have been developed for the earth terrain [1–3]. While all these models aim to predict the brightness temperature or emissivity of a target, the methods vary widely in their approach, complexity, and range of validity. Nowadays, the frequency range of the radiometers used for land applications reaches up to $100 \, \text{GHz}$. However, the theoretical emission models of dry snow are still restricted to a low frequency limit. The aim of this study is to develop a model to describe the emission from dry snow over a wide microwave frequency range. The developed model is based on the radiative transfer equations and the strong fluctuation theory.

Radiative transfer theory describes multiple scattering and transmission of specific intensity in random media [1–3]. The validity criterion for conventional radiative transfer equation is restricted to weak fluctuation and small variance of permittivity. The emissivity of snow is limited to the low-frequency approximation for which the effects of scattering between ice particles are neglected. This limitation means that the emissivity of snow is not dependent on grain size. In order to investigate the properties of snow at high frequencies, the effect of scattering between ice particles must be taken into account. We employ the strong fluctuation theory to solve the problem.

In the strong fluctuation theory, an inhomogeneous layer is modelled as a continuous random medium which can be described by a correlation function. The effective permittivity which depends strongly on the correlation functions is used to characterise the randomness and scattering effects in the layer. The extinction coefficients and the scattering phase functions in the radiative transfer equations also depend strongly on the correlation functions. These correlation functions have relationships with the physical parameters of discrete particles, such as size, shape, etc. In this way, the strong fluctuation theory can be used at high frequencies and the brightness temperature depends on the shape and size of ice particles.

The strong fluctuation theory has been studied using the following correlation functions:

• Spherical symmetric correlation function with exponential form [4–6]:

$$ACF(r) = \exp\left(-\frac{r}{l_s}\right), \tag{1}$$

where l_s is the correlation length.

- Anisotropic correlation function with azimuth symmetric [4, 7]:

$$ACF(r) = \exp\left(-\frac{x^2 + y^2}{l_p^2} - \frac{|z|}{l_z}\right), \tag{2}$$

where $l_p = l_x = l_y$ is the correlation length in horizontal direction and l_z is the correlation length in vertical direction.

- Anisotropic correlation function for ellipsoidal scatters with the form [8–11]:

$$ACF(r) = \exp\left(-\sqrt{\frac{x^2}{l_x^2} + \frac{y^2}{l_y^2} + \frac{z^2}{l_z^2}}\right), \tag{3}$$

where l_x, l_y, and l_z are the correlation lengths in x, y, and z direction, respectively.

Unfortunately, as the same correlation functions are employed by various authors, the effective permittivity and the coefficient $\overline{\overline{S}}$ of the delta function in mean dyadic Green's function are not identical. The key point is that they use a different method to evaluate the principal value of the dyadic Green's function.

In this study, the effective permittivity for a spherical symmetric correlation function with exponential form is used [6]. A detailed discussion on the expressions of the effective permittivity of the spherical symmetric correlation function used by various authors [4, 5] and [6] is given in [6]. A comparison between the measured and the predicted dielectric properties of dry snow shows that the effective permittivity model of Stogryn [6] provides fairly accurate results for the effective permittivity of dry snow in the 18 to 90 GHz range [12]. Furthermore, the coefficient $\overline{\overline{S}}$ of the delta function in the mean dyadic Greens function for the spherical symmetric correlation function has a clear expression [4].

In this paper, the phase matrix and scattering coefficients in the radiative transfer equation for a spherical symmetric correlation function are derived by using the strong fluctuation theory. As a result, we derive a radiative transfer equation which has new constituents and which is applicable to describe multiple scattering, transmission, and thermal emission in strong fluctuating random media. The radiative transfer equations are differential-integral equations which can be solved by using the Gaussian quadrature and eigenanalysis technique

[3, 13]. The brightness temperature of dry snow is calculated and comparisons with literature-based brightness temperature data at 5, 10.7, 18, 37 GHz [14] are presented.

2. FORMULATION

Our microwave emission model for dry snow is based on the solution of the radiative transfer equation inside the snowpack by taking into account boundaries at the soil and atmosphere interfaces (Figure. 1). The model flow chart is shown in Figure. 2.
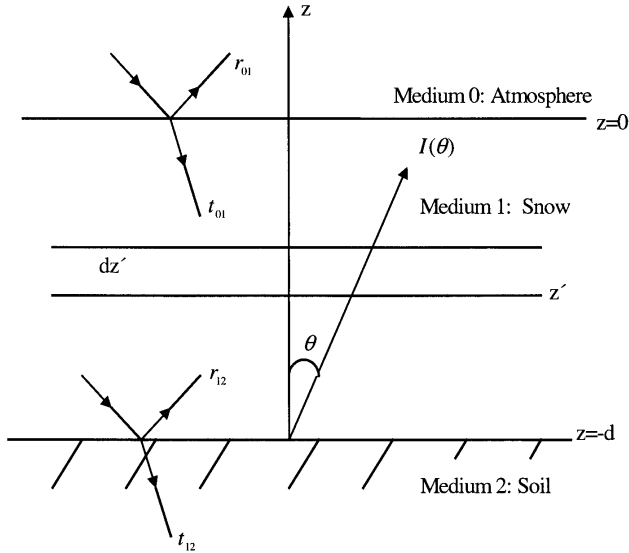
Figure 1. Geometrical configuration of a three-layer medium.

Inside a inhomogeneous medium, let $T_v(\theta, z)$ and $T_h(\theta, z)$ denote brightness temperatures at vertical and horizontal polarisation. The radiation transfer equations for passive remote sensing can be written as [14]:

$$\cos\theta \frac{d}{dz} \begin{bmatrix} T_v(\theta, z) \\ T_h(\theta, z) \end{bmatrix} = \kappa_a T_1(z) - \begin{bmatrix} \kappa_{ev} T_v(\theta, z) \\ \kappa_{eh} T_v(\theta, z) \end{bmatrix}$$
$$+ \int_0^\pi d\theta' \sin\theta' \begin{bmatrix} P_{11}(\theta, \theta') & P_{12}(\theta, \theta') \\ P_{21}(\theta, \theta') & P_{22}(\theta, \theta') \end{bmatrix} \begin{bmatrix} T_v(\theta', z) \\ T_h(\theta', z) \end{bmatrix}, \qquad (4)$$

where κ_a is the absorption coefficient, $\kappa_{ep} = \kappa_a + \kappa_{sp}$ $(p = v, h)$ is the
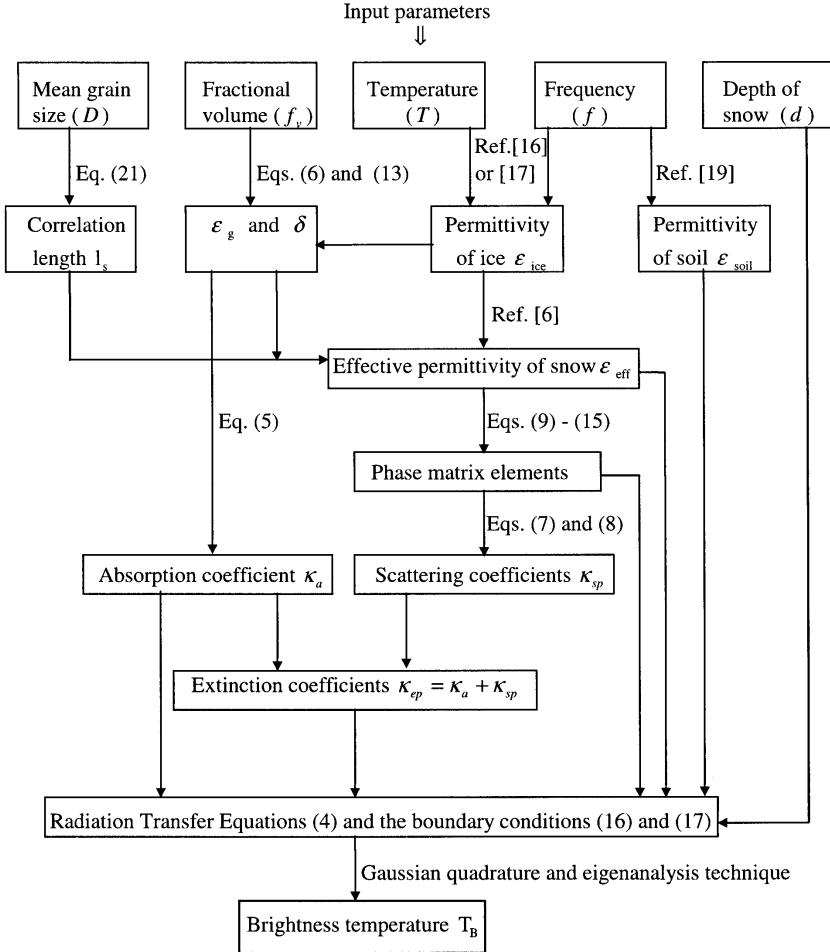
Figure 2. Model structure.

p-polarised extinction coefficient and κ_{sp} is the scattering coefficient. θ is the incidence angle, θ' is the scattering angle, $T_1(z)$ is the temperature profile of the inhomogeneous layer, and $P_{11}(\theta, \theta')$, $P_{12}(\theta, \theta')$, $P_{21}(\theta, \theta')$, $P_{22}(\theta, \theta')$ are the phase matrix elements.

The absorption coefficient κ_a is expressed as [15]:

$$\kappa_a = 2\text{Im}(k_g) = 2k_0\text{Im}\left[\varepsilon_g^{1/2}\right], \tag{5}$$

where k_0 is the wave number in free space, and ε_g is the quasi-static

value of the dielectric constant of dry snow. In the strong fluctuation theory, for a spherical symmetric correlation function, the quasi-static permittivity ε_g is determined by the following equation [4]:

$$f_v \left(\frac{\varepsilon_s - \varepsilon_g}{\varepsilon_s + 2\varepsilon_g} \right) + (1 - f_v) \cdot \left(\frac{\varepsilon_b - \varepsilon_g}{\varepsilon_b + 2\varepsilon_g} \right) = 0, \tag{6}$$

where ε_s is the permittivity of ice particles, $\varepsilon_s = \varepsilon_{ice}$, ε_b is the permittivity of the background, $\varepsilon_b = \varepsilon_0$, f_v is the fraction volume. At VHF, UHF and microwave frequencies (10 MHz–100 GHz), the permittivity of pure and impure ice ε_{ice} can be found in [16, 17].

The scattering coefficients κ_{sv} and κ_{sh} are deduced from the phase matrix components $P(\theta, \phi; \theta', \phi')$ [7]:

$$\kappa_{sv}(\theta) = \int_0^\pi d\theta' \sin\theta' \left[P_{11}(\theta, \theta') + P_{21}(\theta, \theta') \right] \tag{7}$$

$$\kappa_{sh}(\theta) = \int_0^\pi d\theta' \sin\theta' \left[P_{12}(\theta, \theta') + P_{22}(\theta, \theta') \right]. \tag{8}$$

In the strong fluctuation theory, the phase matrix $P(\theta, \phi; \theta', \phi')$ elements are [7]:

$$\begin{aligned} P_{11}(\theta, \theta') = \int_0^{2\pi} d(\phi - \phi') \cdot \delta \big[&\cos^2\theta \cos^2\theta' \cos^2(\phi - \phi') \\ &+ 2\sin\theta \cos\theta \sin\theta' \cos\theta' \cos(\phi - \phi') \\ &+ \sin^2\theta \sin^2\theta' \big] W_{vv}(\theta, \theta'; \phi - \phi') \end{aligned} \tag{9}$$

$$P_{22}(\theta, \theta') = \int_0^{2\pi} d\phi \cdot \delta \cos^2(\phi - \phi') W_{hh}(\theta, \theta'; \phi - \phi') \tag{10}$$

$$P_{12}(\theta, \theta') = \int_0^{2\pi} d\phi \cdot \delta \cos^2\theta \sin^2(\phi - \phi') W_{vh}(\theta, \theta'; \phi - \phi') \tag{11}$$

$$P_{21}(\theta, \theta') = \int_0^{2\pi} d\phi \cdot \delta \cos^2\theta' \sin^2(\phi - \phi') W_{hv}(\theta, \theta'; \phi - \phi'), \tag{12}$$

where δ is the variance of the fluctuation as is for the spherical correlation function [4]

$$\delta = 9 \frac{\varepsilon_g^2}{\varepsilon_0^2} \left[f_v \left(\frac{\varepsilon_s - \varepsilon_g}{\varepsilon_s + 2\varepsilon_g} \right)^2 + (1 - f_v) \cdot \left(\frac{\varepsilon_b - \varepsilon_g}{\varepsilon_b + 2\varepsilon_g} \right)^2 \right]. \tag{13}$$

For the spherical correlation function with exponential form $ACF(r)$ $= \exp\left(-\frac{r}{l_s}\right)$, we have (Appendix and [18]):

$$W_{\alpha,\beta} = \frac{k_{eff}^4 \delta}{2} \frac{1}{\pi} \cdot \frac{l_s^3}{(1+2k_{eff}^2[1-\cos\theta\cos\theta'-\sin\theta\sin\theta'\cos(\phi-\phi')]l_s^2)^{3/2}}$$

$$\cdot \cos\left[3\arctan\left(k_{eff}\sqrt{2}[1-\cos\theta\cos\theta'-\sin\theta\sin\theta'\cos(\phi-\phi')]^{1/2}l_s\right)\right], (14)$$

where the wave number k_{eff} is:

$$k_{eff} = \omega\sqrt{\mu\varepsilon_{eff}} = k_0\sqrt{\frac{\varepsilon_{eff}}{\varepsilon_0}}, \tag{15}$$

where ε_{eff} is the effective permittivity of snow layer. In this study, the effective permittivity of dry snow for a spherical symmetric correlation function with exponential form is used [6].

The radiative transfer equation (4) can be solved by using Gaussian quadrature and eigenanalysis technique subject to the following boundary conditions, for $0 < \theta < \pi/2$ [13]:

$$T_p(\theta, z = -d) = r_{12p}(\theta)T_p(\pi - \theta, z = -d) + t_{12p}(\theta)T_{soil} \tag{16}$$
$$T_p(\pi - \theta, z = 0) = r_{01p}(\theta)T_p(\theta, z = 0) + t_{01p}(\theta)T_{skyp}(\theta_0), \tag{17}$$

where r_{12p}, r_{01p} are reflectivities, t_{12p}, t_{01p} are transmissivities, and $t_{mnp} = 1 - r_{mnp} \cdot \theta$ and θ_0, and θ and θ_2 are related by Snells law, respectively.

In the calculation of the reflectivity, the effective permittivity of snow layer and soil should be known. In this study, the Stogryns model in [6] is used to calculate the effective permittivity of dry snow. The measured permittivity and dielectric loss factor of soil as a function of frequency with temperature as a parameter can be obtained from [19].

The sky radiation is approximated by [13]:

$$T_{skyp}(\theta_0) = T_{air}\left[1 - \exp(-k_{0a} \cdot t \cdot \sec\theta_0)\right] \tag{18}$$

with T_{air} denoting the air temperature, k_{0a} the absorption coefficient of air, and t the thickness of the atmosphere.

Once the radiation transfer equation (4) is solved subject to the boundary conditions (16) and (17), the brightness temperatures are given by [13]:

$$T_B(\theta_0) = t_{01p}(\theta)T_p(\theta, z = 0) + r_{01p}(\theta_0)T_{skyp}(\theta_0). \tag{19}$$

To find a possible effect due to the small roughness of the surface, we simply modify the reflectivity r_{mnp} according to [7]:

$$r_{mnp1} = \exp(-h \cos^2 \theta) r_{mnp} \tag{20}$$

where h is the effective roughness.

3. COMPARISON WITH OTHER MODELLING APPROACHES AND EXPERIMENTAL DATA

Here we show the results for interpretation of experimental data collected from a snow field [14] by using the microwave emission model developed in this study. For convenience, we call this model as Continuous Media Model (CM). Comparisons with the results of First-Order Radiative Transfer Solution (FOM) [2] and Discrete Spherical Scatterer Model (DM) [3] are also shown.

In [14], a set of four microwave radiometers operating at frequencies 5, 10.7, 18 and 37 GHz were used to measure the brightness temperatures of a snow field. The only two ground truth data included are the depth $(d = 66\,\mathrm{cm})$ and the temperature $(T = 272\,\mathrm{K})$ of the snowpack. Other input parameters, such as the mean grain size, fraction volume, and permittivity of the snowpack, are not available from the study. In spite of this, we choose this date set, because in [2, 3], First-Order Radiative Transfer Solution (FOM) and Discrete Spherical Scatterer Model (DM) were used to interpret the same experimental data. For each model, the unknown parameters are selected in such a way that the model result fits into the experimental data. This is why that these various models fit the experimental data well as shown in Figures 3–6, but the input parameters are so different in various references as shown in Table 1 ([1–3, 14]).

The input parameters of the Continuous Media Model (CM) for dry snow are the measurement frequency, the temperature of snow, the depth of snow, the mean grain size of ice particles and the volume fraction of ice particles. The relationship between the mean grain size D and the correlation length l_s is [21]

$$l_s = 0.85 \frac{D}{3}. \tag{21}$$

In the calculation, the input parameters of the Continuous Media Model (CM) are based on measurement data except the mean grain
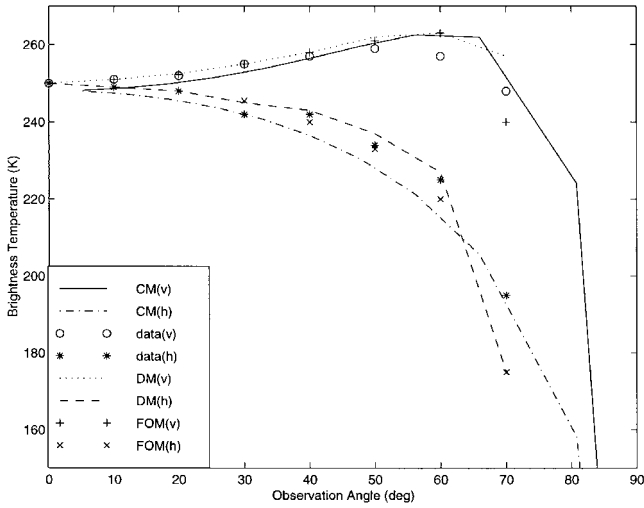
Figure 3. Comparison of CM with experimental emissivity values given in [14] at 5 GHz. Comparisons with FOM [2] and DM [3] are also presented.
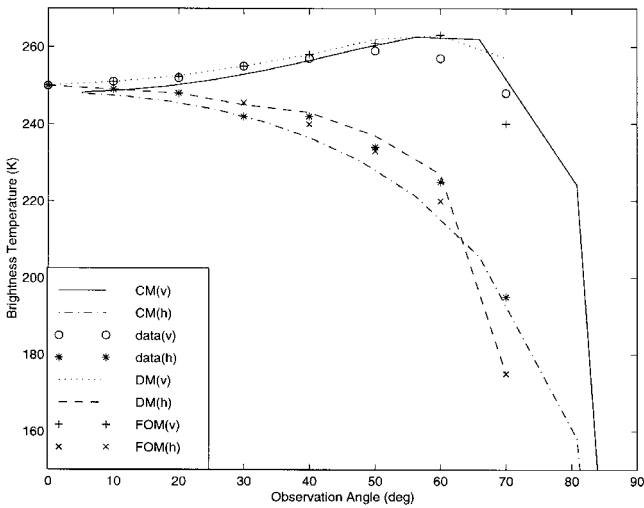
Figure 4. Comparison of CM with experimental emissivity values given in [14] at 10.7 GHz. Comparisons with FOM [2] and DM [3] are also presented.
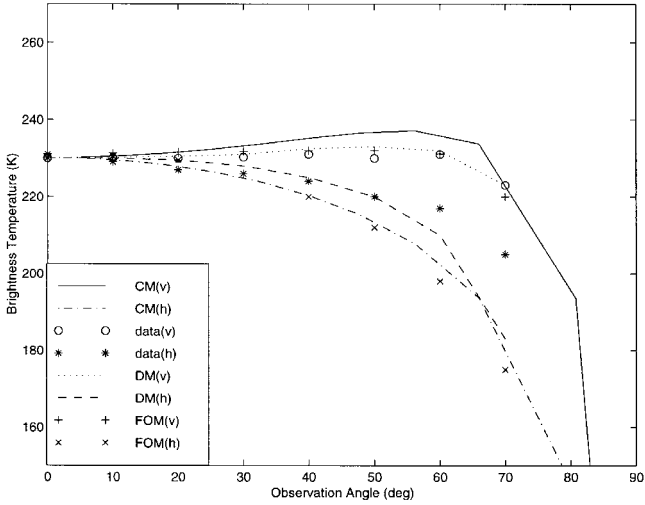
Figure 5. Comparison of CM with experimental emissivity values given in [14] at 18 GHz. Comparisons with FOM [2] and DM [3] are also presented.
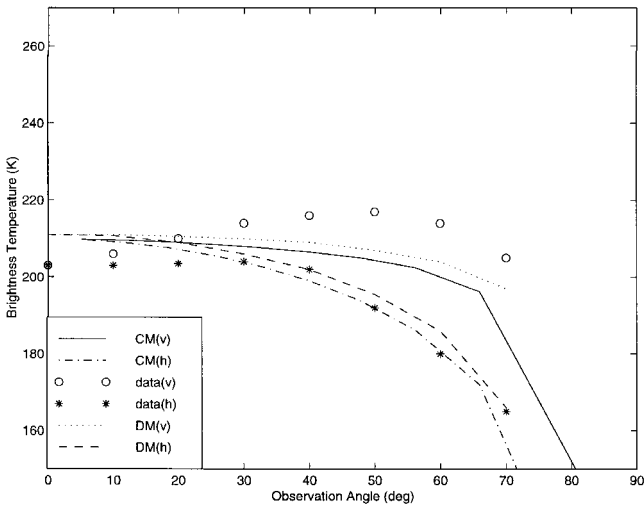
Figure 6. Comparison of CM with experimental emissivity values given in [14] at 37 GHz. Comparisons with FOM [2] and DM [3] are also presented.

Table 1. Continuous Media Model (CM) parameters in order to fit model prediction into experimental data [14] at (a) 5 GHz, (b) 10.7 GHz, (c) 18 GHz, and (d) 35 GHz. First Order Radiative Transfer Solution (FOM) input parameters are obtained from [2] and Discrete Spherical Scatterer Model (DM) input parameters from [3], respectively.

Model	D (mm)	f_v	d (cm)	ε_{ice}	ε_{eff} (now)	ε_{soil}	Albedo
CM	0.8	0.3	66	3.15+0.0004i	1.467+0.00010i	5.0+0.5i	
FOM	1.7	0.3	66		1.476+0.00210i	5.0	0.05
DM	3.5	0.083	66	3.20+0.0005i	1.500+0.00375i	6.0+0.6i	

(a)

Model	D (mm)	f_v	d (cm)	ε_{ice}	ε_{eff} (now)	ε_{soil}	Albedo
CM	0.8	0.3	66	3.15+0.0009i	1.4688+0.00050i	5.0+0.6i	
FOM	1.7	0.3	66		1.4745+0.00245i	5.0	0.2
DM	3.5	0.083	66	3.20+0.0005i	1.5000+0.00375i	6.0+0.6i	

(b)

Model	D (mm)	f_v	d (cm)	ε_{ice}	ε_{eff} (now)	ε_{soil}	Albedo
CM	0.8	0.3	66	3.15+0.0016i	1.4728+0.00190i	5.0+0.5i	
FOM	1.7	0.3	66		1.4700+0.00212i	4.0	0.2
DM	3.5	0.083	66	3.20+0.0005i	1.5000+0.00375i	6.0+0.6i	

(c)

Model	D (mm)	f_v	d (cm)	ε_{ice}	ε_{eff} (now)	ε_{soil}
CM	0.8	0.3	66	3.15+0.0032i	1.4884+0.01210i	5.0+0.4i
DM	3.5	0.083	66	3.20+0.0005i	1.5000+0.00375i	6.0+0.6i

(d)

size and the fraction volume. The other parameters, such as the ice permittivity ε_{ice}, the effective permittivity of snow ε_{eff} are calculated from the models [6, 16, 17]. The permittivity of soil ε_{soil} is obtained from [19].

The parameters used with different models at 5, 10.7, 18 and 37 GHz are shown in Table 1. The First-Order Radiative Transfer Solution (FOM) and Discrete Spherical Scatterer Model (DM) input parameters as well as model predictions are obtained from [2, 3], respectively. At

37 GHz, FOM data are not available in [2]. This is because this simple model is not suitable for cases where multiple scattering is significant [2].

Table 1 shows that in order to fit experimental data, the Discrete Spherical Scatter Model (DM) requires the use of a larger grain size ($D = 3.5$ mm) and smaller volume fraction ($f_v = 0.083$) than the other two models. In the Continuous Media Model (CM), we used the more realistic value than DM for the grain size ($D = 0.8$ mm) and the volume fraction ($f_v = 0.3$) for the dry snow case.

The ice permittivity ε_{ice} for CM and DM are almost same at 5 GHz. The value of ice permittivity ε_{ice} at 5 GHz is used also for 10.7, 18 and 37 GHz in DM [3]. In the Continuous Media Model (CM), the ice permittivity ε_{ice} is calculated from the model [16] or [17]. Hence, the imaginary part of ε_{ice} is dependent on frequency.

The effective permittivity of snow ε_{eff} is quite different for various models. References [1–3, 14] do not mention which model for the effective permittivity of snow ε_{eff} is used. In the case of DM predictions, the same values of effective permittivity of snow ε_{eff} are used for 5, 10.7, 18 and 37 GHz in DM. In the case of Continuous Media Model (CM), ε_{eff} is calculated according to [7]. Thus, the real part of ε_{eff} is correctly dependent on frequency, whereas its imaginary part increases strongly with increasing frequency.

The angular dependence of the brightness temperature was calculated by using the Continuous Media Model (CM) at the four frequencies. The results are presented in Figs. 3–6. For comparison, the experimental data [11] and results from the other two models (DM, FOM) [2, 3] are also given in Figs. 3–6. The results show that the agreement between the model predictions and measurements is good. In Fig. 7, the brightness temperatures are plotted as a function of frequency for the viewing angle of 33 degrees off nadir.

The initial motivation to develop our new model is to investigate the properties of snow at high microwave frequencies. As we discussed earlier in this section, FOM data are not available at 37 GHz in [2], whereas our model can work very well at 37 GHz. Unfortunately, there are no experimental angular dependence data for the brightness temperature of the dry snow at higher frequencies up to date. The effective permittivity and the extinction coefficients are the important parts of our new model. Our previous studies have shown that the effective permittivity model used here provides reasonably accurate results for
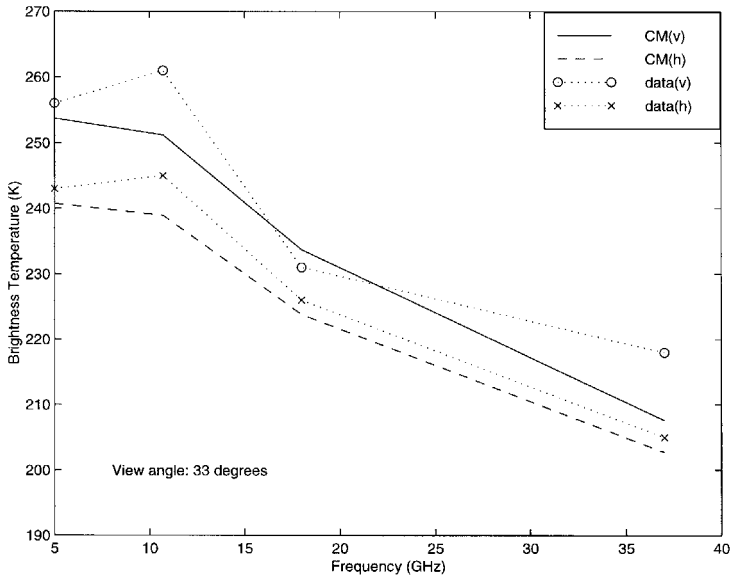
Figure 7. Brightness temperature as a function of frequency according to CM predictions and experimental data.

the imaginary part of the effective permittivity in the 1 to 100 GHz range except for large grain sizes at high frequencies (60 to 90 GHz) [12], and the extinction coefficient model predictions agree well with the measured extinction coefficients for 35 GHz and 60 GHz and for grain sizes smaller than 0.9 mm at 90 GHz [18]. Thus, we can expect that our model for the brightness temperature can work up to 60 GHz, and up to 90 GHz for small grain sizes ($D < 0.9$ mm). Of course, this conclusion needs to be tested once we have the experimental data at those high frequencies.

4. CONCLUSIONS

In this study, an emission model for dry snow is derived by using radiative transfer equations and the strong fluctuation theory. The input parameters of the model are frequency, temperature, snow depth, mean grain size of ice particles, and the volume fraction of the ice particles.

Interpretation of experimental data collected from a snow field [14] was made. It was shown that the model predictions agree well with the experimental data in the frequency range from 5 to 37 GHz. The values of input parameters for CM for the grain size ($D = 0.8\,\mathrm{mm}$) and the volume fraction ($f_v = 0.3$) are more realistic than those of DM [3]. In our model, the ice permittivity ε_{ice}, the effective permittivity of snow ε_{ice}, and the permittivity of soil ε_{soil} are dependent on the frequencies, whereas those parameters of the DM are the same for all frequencies. FOM data are not available at 37 GHz in [2], whereas our model can work very well at 37 GHz, and we can expect that it can work up to 60 GHz, and up to 90 GHz for small grain sizes ($D < 0.9\,\mathrm{mm}$).

APPENDIX. THE DERIVATION OF PARAMETER $W_{\alpha,\beta}$

The calculation of the function $W_{\alpha,\beta}$ (see (14)) is started from [3]

$$W_{\alpha,\beta} = \frac{\pi k_{eff}^4 \delta}{2} \Phi\left(k_{eff}(\hat{k}_i - \hat{k}_s)\right), \tag{A1}$$

where k_{eff} is the effective wave number in snow, $\hat{k}_i$ is the incident direction of incident plane wave, and $\hat{k}_s$ is the scattered direction of scattered wave. The $\hat{k}_i - \hat{k}_s$ in (A1) can be written in terms of $(\theta, \phi; \theta', \phi')$ as:

$$\hat{k}_i - \hat{k}_s = \Big[(\sin\theta\cos\theta - \sin\theta'\cos\theta')^2$$

$$+ (\sin\theta\sin\phi - \sin\theta'\sin\phi')^2 + (\cos\theta - \cos\theta')^2\Big]^{1/2}$$

$$= \sqrt{2}\left[1 - \cos\theta\cos\theta' - \sin\theta\sin\theta'\cos(\phi - \phi')\right]^{1/2}. \tag{A2}$$

In (A1), Φ is the spectral density function, which is defined as the three-dimensional Fourier transform of the normalised correlation function $ACF(\bar{r}' - \bar{r}'')$

$$\Phi\left(\bar{k}\right) = \frac{1}{8\pi^3} \int_{-\infty}^{\infty} d^3\bar{r}\, ACF(\bar{r}) e^{i\bar{k}\cdot\bar{r}}. \tag{A3}$$

In the spherical symmetric case with exponential correlation function [4]:

$$ACF(|\bar{r}|) = \exp\left(-\frac{|\bar{r}|}{l_s}\right), \tag{A4}$$

where l_s is correlation length. By substituting (A4) into (A3), we obtain:

$$\Phi(\bar{k}) = \frac{1}{8\pi^3} \int_{-\infty}^{\infty} d^3\bar{r} \exp\left(\frac{|\bar{r}|}{l_s}\right) e^{i\bar{k}\cdot\bar{r}}$$

$$= \frac{1}{8\pi^3} \int_0^{2\pi} d\phi \int_0^{\pi} \sin\theta d\theta \int_{-\infty}^{\infty} dr \; r^2 \exp\left(-\frac{r}{l_s}\right) e^{ikr}$$

$$= \frac{1}{8\pi^3} \cdot 2\pi \cdot 2 \cdot \int_{-\infty}^{\infty} dr \; r^2 \exp\left(-\frac{r}{l_s}\right) e^{ikr}. \tag{A5}$$

The integral in (A5) is a one-dimensional Fourier transform of the function $f(r) = f^2 \exp\left(-r/l_s\right)$ and the result is [20]:

$$\int_{-\infty}^{\infty} dr \; r^2 \exp\left(-\frac{r}{l_s}\right) e^{ikr} = 2l_s^3 \Gamma(3) \frac{1}{(1+k^2 l_s^2)^{3/2}} \cos\left[3\arctan\left(kl_s\right)\right], \tag{A6}$$

where the Gamma function $\Gamma(3) = 2 \cdot$ $W_{\alpha,\beta}$ can be written as:

$$W_{\alpha,\beta} = \frac{\pi k_{eff}^4 \delta}{2} \cdot \frac{1}{\pi^2} \cdot \frac{l_s^3}{\left(1 + \left[k_{eff}\left(\hat{k}_i - \hat{k}_s\right)\right]^2 l_s^2\right)^{3/2}}$$

$$\cdot \cos\left[3\arctan\left(k_{eff}\left(\hat{k}_i - \hat{k}_s\right) l_s\right)\right]. \tag{A7}$$

By substituting (A2) into (A7), we obtain:

$$W_{\alpha,\beta} = \frac{k_{eff}^4 \delta}{2} \cdot \frac{1}{\pi} \cdot \frac{l_s^3}{\left(1 + 2k_{eff}^2 \left[1 - \cos\theta\cos\theta' - \sin\theta\sin\theta'\cos\left(\phi-\phi'\right)\right] l_s^2\right)^{3/2}}$$

$$\cdot \cos\left[3\arctan\left(k_{eff}\sqrt{2}[1 - \cos\theta\cos\theta' - \sin\theta\sin\theta'\cos\left(\phi-\phi'\right)^{1/2} l_s\right)\right]. \tag{A8}$$

REFERENCES

1. Ulaby, F., R. Moore, and A. Fung, *Microwave Remote Sensing*, Vol. III, Artech House, Inc., Norwood, MA, 1986.
2. Fung, A. K., *Microwave Scattering and Emission Models and Their Applications*, Artech House, 1994.
3. Tsang, L., J. A. Kong, and R. T. Shin, *Theory of Remote Sensing*, Wiley Series in Remote Sensing, J. A. Kong (ed.), New York, 1985.

4. Tsang, L., and J. A. Kong, "Scattering of electromagnetic waves for random media with strong permittivity fluctuations," *Radio Sci.,* Vol. 16, 303–320, 1981.

5. Tsang, L., J. A. Kong, and R. W. Newton, "Application of strong fluctuation random medium theory to scattering of electromagnetic waves from a half-space of dielectric mixture," *IEEE Trans. on Antennas and Propagation,* Vol. 30, No. 2, 292–302, 1982.

6. Stogryn, A., "The bilocal approximation for the effective dielectric constant of an isotropic random medium," *IEEE Trans. on Antennas and Propagation,* Vol. 32, No. 5, 517–520, 1984.

7. Jin, Y. Q., "The radiative transfer equation for strongly-fluctuation continuous random media," *J. Quant. Spectrosc. Radiat. Transfer,* Vol. 42, 529–537, 1989.

8. Nghiem, S. V., R. Kwok, J. A. Kong, and R. T. Shin, "A model with ellipsoidal scatters for polarimetric remote sensing of anisotropic layered media," *Radio Sci.,* Vol. 28, 687–703, 1993.

9. Nghiem, S. V., R. Kwok, S. H. Yueh, J. A. Kong, C. C. Hsu, M. A. Tassoudji, and R. T. Shin, "Polarimetric scattering from layered media with multiple species of scatterers," *Radio Sci.,* Vol. 30, 835–852, 1995.

10. Nghiem, S. V., R. Kwok, J. A. Kong, R. T. Shin, S. A. Arcone, and A. J. Gow, "An electrotheromdynamic model with distributed properties for effective permittivity of sea ice," *Radio Sci.,* Vol. 31, 297–311, 1996.

11. Yueh, S. H., and J. A. Kong, "Scattering from random oriented scatters with strong permittivity fluctuations," *J. Electrom. Waves and Appl.,* Vol. 4, 983–1004, 1990.

12. Wang, H., J. Pulliainen, and M. Hallikainen, "Effective permittivity of dry snow in the 18 to 90 GHz range," *J. Electrom. Waves and Appl.,* Vol. 13, 1391–1392, 1999 for abstract; *Progress in Electromagnetics Research,* PIER 24, 119–133, 1999 for the complete text.

13. Tsang L., and J. A. Kong,, "Thermal microwave emission from a three-layer random medium with three-dimensional variations," *IEEE Trans. Geosci. Remote Sensing,* Vol. 18, No. 2, 212–216, 1980.

14. Kong, J. A., R. Shin, J. Shiue, and L. Tsang, "Theory and experiment for passive microwave remote sensing of snowpacks," *J. Geophys. Res.,* Vol. 48, No. B10, 5669–5673, 1979.

15. Hallikainen, M., F. Ulaby, and T. Van Deventer, "Extinction behaviour of dry snow in the 18- to 90-GHz range," *IEEE Trans. Geosci. Remote Sensing,* Vol. 25, No. 6, 737–745, 1987.

16. Hufford, G., "A model for the complex permittivity of ice at frequencies below 1 THz," *International Journal of Infrared and Millimeter Waves,* Vol. 12, No. 7, 677–682, 1991.

17. Mätzler, C., and U. Wegmüller, "Dielectric properties of fresh-water ice at microwave frequencies," *J. Phys. D: Appl. Phys.,* Vol. 20, 1623–1630, 1987.

18. Wang, H., J. Pulliainen, and M. Hallikainen, "Extinction behaviour of dry snow at microwave range up to 90 GHz by using strong fluctuation theory," *1998 IEEE International Geoscience and Remote Sensing Symposium Proceedings,* 42–44, Seattle, WA, USA, June 6–10, 1998.

19. Hallikainen, M., F. Ulaby, M. Dobson, M. El-Rayes, and L. Wu, "Microwave dielectric behaviour of wet soil — Part I: Empirical equations and experimental observations," *IEEE Trans. on Geosci. Remote Sensing,* Vol. 23, No. 1, 25–34, 1985.

20. Oberhettinger, F., *Fourier Transforms of Distributions and Their Inverses, A Collection of Tables,* Academic Press, Inc., New York, 1973.

21. Wang, H., J. Pulliainen, and M. Hallikainen, "Correlation functions and correlation lengths for dry snow," *J. Electrom. Waves and Appl.,* Vol. 12, 1337–1347, 1998.